

### **3.3.3 A Comparison of Fischer-Tropsch Synthesis in a Slurry Bubble Column Reactor and a Continuous Stirred Tank Reactor**

#### **Abstract**

Fischer-Tropsch synthesis (FTS) was studied using a precipitated Fe/K catalyst in a improved short slurry bubble column reactor (SBCR) equipped with a satisfactory reactor-wax separation system and a continuous stirred tank reactor (CSTR) using the same experiment conditions. The catalyst in the SBCR had a lower catalytic activity. Methane and the products of the gas are higher in the CSTR. Some effects may be related to different mixing heat, mass transfer phenomena between two reactors. The  $C_3+$  hydrocarbons ( $C_3+H.C.$ ) with synthesis gas ( $CO+H_2$ ) conversion ratio had similar values.

#### **Introduction**

A SBCR is a gas-liquid-solid reactor in which the finely divided solid catalyst is suspended in the liquid by the rising gas bubbles. It offered the following advantages: (a) the ability of the liquid phase to handle the large heats of reaction, (b) low  $H_2/CO$  ratio synthesis gas without needing a preliminary water-gas shift step, and (c) relatively low capital and operating cost. A considerable interest has been expressed in using the SBCR to carry out FTS.

FTS takes place in a SBCR where the synthesis gas is converted on catalysts suspended in a liquid as fine particles. The synthesis gas flows as small bubbles through the catalyst suspension. The products are volatile under the synthesis conditions which are removed with unconverted gases, and the liquid products are separated from the suspension. The bubbles in the reactor are produced by the gas distributor located in the bottom of the reactor. As reported by W-D Deckwer, et al. (1),

the higher liquid phase transfer coefficient values were found in short columns, and it can be explained with the increased mass transfer during bubble formation, but the formation of the bubble should be regarded as end effect which will be constant for a given gas distributor. The engineering problem for bubble column reactor that needed to be solved was the catalyst separation from wax.

The improved design of the short bubble column reactor in CAER F-T pilot unit contains a good axial dispersion function and a continuous reactor-wax removal system. This axial dispersion function would cause an increase in gas-liquid backmixing, and would have a great effect on conversion and selectivity. The improved F-T reactor-wax separation system enabled us to increase the flexibility and reduce the manpower requirement for the reactor-wax/slurry separation.

A CSTR is designed to use a powdered catalyst in a slurry. The agitation of the reactor provides optimum isothermal and residence time conditions. A dip-tube fitted inside the reactor provides excellent gas/liquid contact.

The purpose of the present study was to compare certain aspects of the FTS as carried out on the same precipitated Fe/K catalyst in the SBCR and the CSTR using the same experimental conditions. It is expected that there would be some differences in the conversion and selectivities obtained from these reactors, because these reactors differ in the type of mixing and heat and mass transfer phenomena.

## **Experimental**

A schematic diagram of the experimental apparatus is shown in Figure 1 for the SBCR and Figure 2 for the CSTR. The bubble column reactor has 5.08 cm diameter and a 2 m height. The CSTR is 1 liter autoclave. The SBCR was equipped with a gas distributor and a K-ray detector. The gas distributor produce fine gas bubbles in the

liquid phase and the K-ray indicates the catalyst axial suspension inside the reactor. The CSTR was filled initially about 2/3 of the reactor volume and the SBCR filled about 3/4 of the column volume with the slurry that was made of 20 wt% catalyst and the Shell C<sub>30</sub> oil. The level of the slurry is dependent on the calculation of gas holdup in the SBCR at the synthesis condition (2). Briefly, the synthesis gas was passed continuously through the reactors, the products gas and liquid, at the top of the reactor pass through a separation section to a hot condenser (230°C), and a cold separator (3°C). A dry flow meter for SBCR and a bubble meter for CSTR was used to measure the exit gas flow rate.

The composition of the exit gas was determined by GC techniques. The condensed liquid phases were sampled at periodic times (12 hours for SBCR and 24 hours for CSTR) and the mass of each sample was obtained. The aqueous phase was analyzed for water and oxygenates using a GC fitted with Porpack Q column. The oil and wax phases sample was combined according to the mass fraction, O-xylene was added as an internal standard, then this sample was analyzed for hydrocarbons by GC with the DB-5 column.

The catalyst particle sizes after synthesis for 309 hours (SBCR) and for 253 hours (CSTR) were obtained by SEM. The SEM was carried out after coating the power samples with carbon, using a Hitachi S-2700 scanning electron microscope at 20 KV. EDS was carried out using a thin window Si-Li diode detector.

The operating conditions for both reactor systems are given in Table 1.

## **Results and Discussion**

### **Catalyst axial dispersion and mixing**

The gas-liquid backmixing plays an important role in the performance of the reactor. The quality of the flow is dependent on the type of gas distributor, properties of the liquid, column size, gas velocities, solid concentration and solid particle (3-5). At low gas velocity (<5 cm/sec.), the bubble rise separately in the liquid or slurry and the homogeneous bubble flow regime prevails (3). The solid dispersion, detected by a K-ray at gas velocity 3 cm/sec, shows that the liquid phase is more likely uniform in the column (Figure 3). However, a trend towards bubble coalescence behavior was also observed in this figure. The agitation in the SBCR by rising gas bubbles and in the CSTR by a magnedrive stirrer operated at 750 rpm, so that the agitation of the CSTR provides excellent mixing.

### **Conversion**

Table 2 lists the data obtained from the both reactor systems at same time-on-stream time. It is shown that the difference in conversion between the two reactors is caused by the difference of heat and mass transfer phenomena and gas resident time in the reactor. The gas hourly space velocity (GHSV) based on the volume of reactor is 379 in the SBCR and 209 in the CSTR. Some possible effects of the reactor type on the catalyst activity may be caused by the GHSV based on the liquid volume is slight different (518 in the SBCR and 504 in the CSTR) and the liquid level is much higher in the SBCR, the synthesis products volatile under the operating conditions are removed slowly with the residual gas in the SBCR, so that some high molecular weight liquid products remain in the reactor, fill catalyst pores, and surround the catalyst particles (6). The  $H_2O/H_2$  ratio is slightly higher in the SBCR. This can produce the iron and iron

carbides present as magnetite (7,8). Therefore, maximum F-T conversion may be influenced by the reaction of iron carbide with  $H_2O$  to form  $Fe_3O_4$ , which has no hydrocarbon synthesis activity. A possible explanation of the observed deactivation could be carbon formation as result of the Boudouard reaction. Carbon deposition in the SBCR causes disintegration of catalyst particles to fines. Apparently, carbon nuclei form inside the Fe crystallites and grow to an extent that the particles are broken by the expanding carbon deposit (Figure 5) (9). The mechanically stirring in the CSTR disintegrates the catalyst particles to fines (Figure 6).

### Selectivity

The production of methane is slight higher in the CSTR, and the  $C_3$ - $C_4$  olefin/paraffin ratio is not significantly different in the two systems. The gas production is higher in the CSTR ( 84.4% and 80.6%), because the water gas shift reaction is stronger in the CSTR. The  $C_3$ + H.C. (g/ $M^3$ -hr)/CO+ $H_2$  conversion ratio is almost same in the two systems (1.63 in the SBCR and 1.65 in the CSTR). Figure 7 illustrates the differences in the products distributions for both reactors. The mole fraction of higher molecular weight products is higher in the SBCR, and the plot of the products breaks sharply at about  $C_{12}$ . The alpha values based on total hydrocarbons formation for the SBCR, are 0.68 and 0.93, and for the CSTR, are 0.42 and 0.82. After 240 hours on-stream, the carbon number distributions are similar for both reactors (Figure 8).

### Summary

The improved design of the CAER short bubble column reactor offers good gas-slurry mixing and excellent catalyst wax separations. The iron concentration in the wax collected after passing the separation system is about 10 ppm. The data presented in this study indicate that the catalyst activity is different between two reactor systems at

same operating conditions, the activity is about 10% higher in the CSTR than in the SBCR, the water-gas shift reaction is weak and the gas percentage of synthesis products is less in the SBCR, the  $(C_1+C_2)$ /total hydrocarbons ratio is higher in the SBCR. The SBCR produced more the higher molecular weight products on-stream for synthesis times of less than 240 hours.

## References

1. D. Deckwer, R. Burckhart and G. Zoll, 1974. Chemical Engineering Science, 29, 2177.
2. J. M. Fox and B. D. Degen, 1990. U.S. DOE Report, No.PC89867-T1.
3. Shigeharu Morooka, Tetsuya Mizoguchi, Tokihiro Kago and Yasuo Kato, 1986. Journal of Chemical Engineering of Japan, 19, 6.
4. Serap Kara, Balmohan G. Kelkar, and Yatish T. Shah, 1982. Ind. Eng. Chem. Process Des. Dev., 21, 584.
5. Yasuo Kato, Akio Nishiwaki, Takashi Fukuda and Shigenobu Tanaka, 1972. Journal of Chemical Engineering of Japan, 5, 2.
6. Charles N. Satterfield, George A. Huff, Jr., and Harvey G. Stenger, 1985. Ind. Eng. Chem. Fundam, 24, 450.
7. Robert Bernard Anderson, 1984. "The Fischer-Tropsch Synthesis" Academic Press, Inc.
8. R.D. Srivastava, Burns and Roe Services Corp. And V.U. S. Rao, G. Cinguegrane and G. J. Stiegel, 1990. Hydrocarbon Processing, 69,59.
9. Charles N. Satterfield and Harvey G. Stenger, 1984. Ind. Eng. Chem. Process Des. Dev. 23,26.

Table 1		
Operating Conditions		
	SBCR(503)	CSTR(LX238)
Catalyst	4.4 Si/K	4.4 Si/K
Cat. loaded wt%	20	20
Cat. Activation at:		
Gases	CO+H <sub>2</sub>	CO+H <sub>2</sub>
H <sub>2</sub> /CO	0.7	0.7
Gas space velocity (SL/hr-g Fe)	5.3	5.15
Temperature (°C)	270	270
Pressure (atm.)	1	1
Synthesis at:		
H <sub>2</sub> /CO	0.7	0.7
Gas space velocity (SL/hr-g Fe)	5.3	5.15
Temperature (°C)	270	270
Pressure (MPa)	1.21	1.21
Gas superficial velocity (cm/sec)	3	Stirred speed 750 RPM



Table 2		
Conversion and Selectivity		
	SBCR	CSTR
CO Conversion %	48.63	58.94
H <sub>2</sub> Conversion %	48.38	54.52
CO+H <sub>2</sub> Conversion %	48.48	57.03
Products gas (%)	80.63	84.44
(C <sub>1</sub> +C <sub>2</sub> )/T.H.C. (%)	16.76	15.45
C <sub>2</sub> /(C <sub>2</sub> +C <sub>2=</sub> ) (%)	45.01	48.66
C <sub>3</sub> /(C <sub>3</sub> +C <sub>3=</sub> ) (%)	87.03	87.99
C <sub>4</sub> /(C <sub>4</sub> +C <sub>4=</sub> ) (%)	84.27	84.23
C <sub>3</sub> +H.C.(g/M <sub>3</sub> -hr)/CO+H <sub>2</sub> (%) Conversion	1.63	1.65
H <sub>2</sub> O/H <sub>2</sub> Ratio	1.26	1.2
H <sub>2</sub> /CO Usage	0.69	0.67

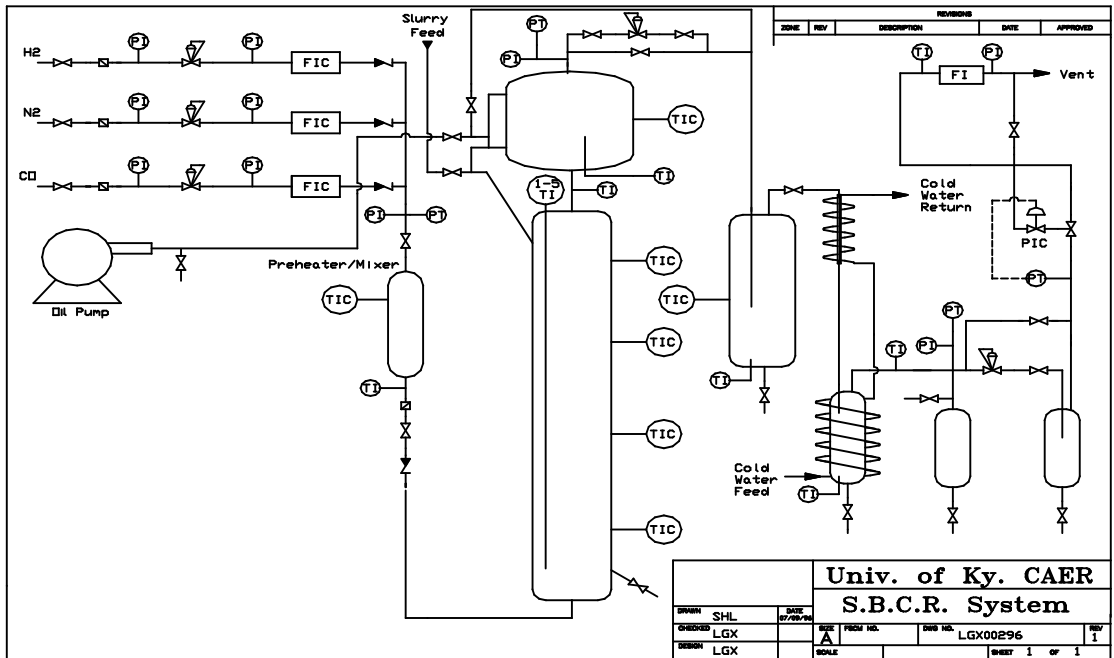


Figure 1. Schematic of the FTS slurry bubble column reactor.

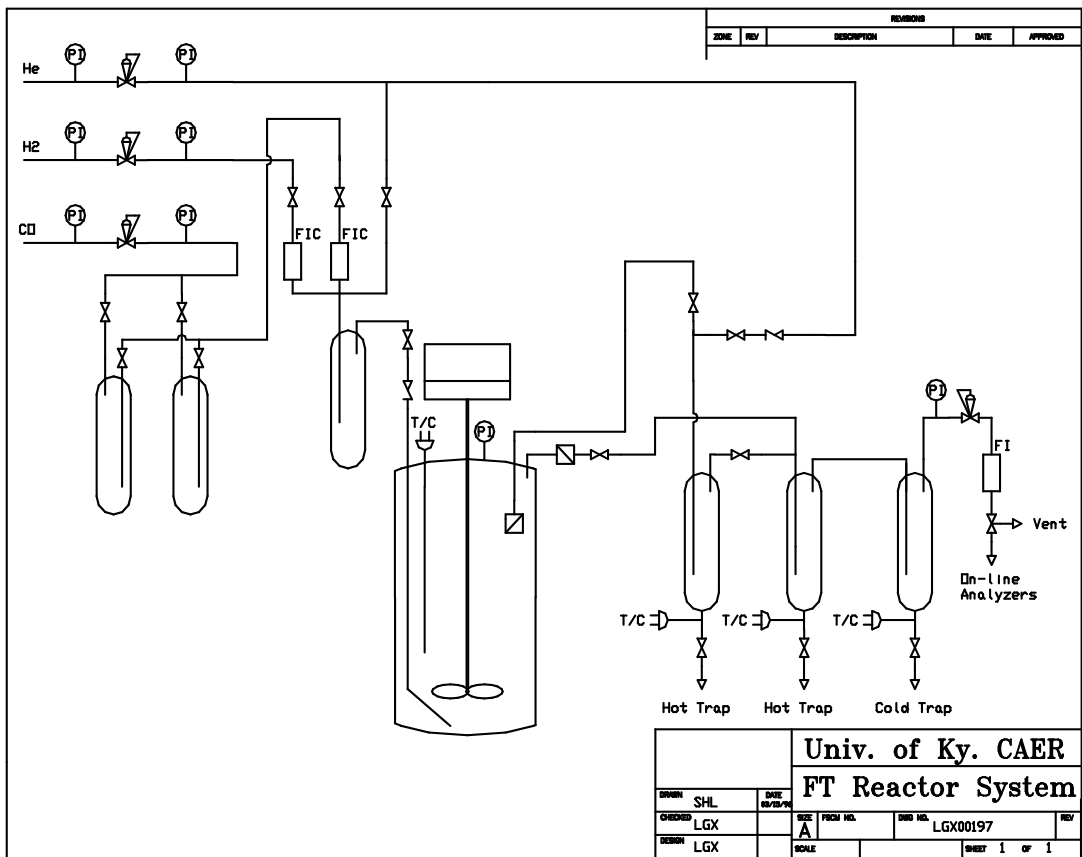


Figure 2. Schematic of the CSTR FTS reactor system.

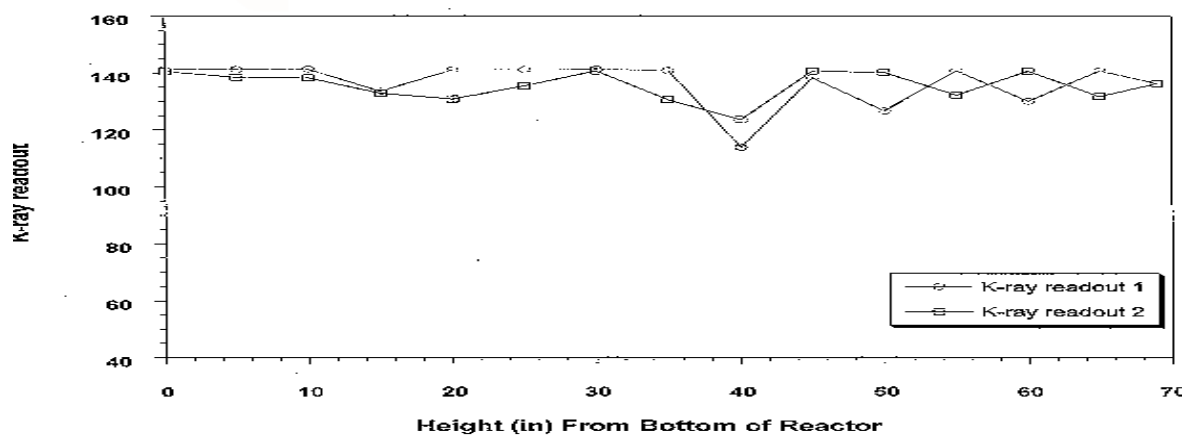


Figure 3. K-ray data for the SBCR indicating uniform catalyst distribution.

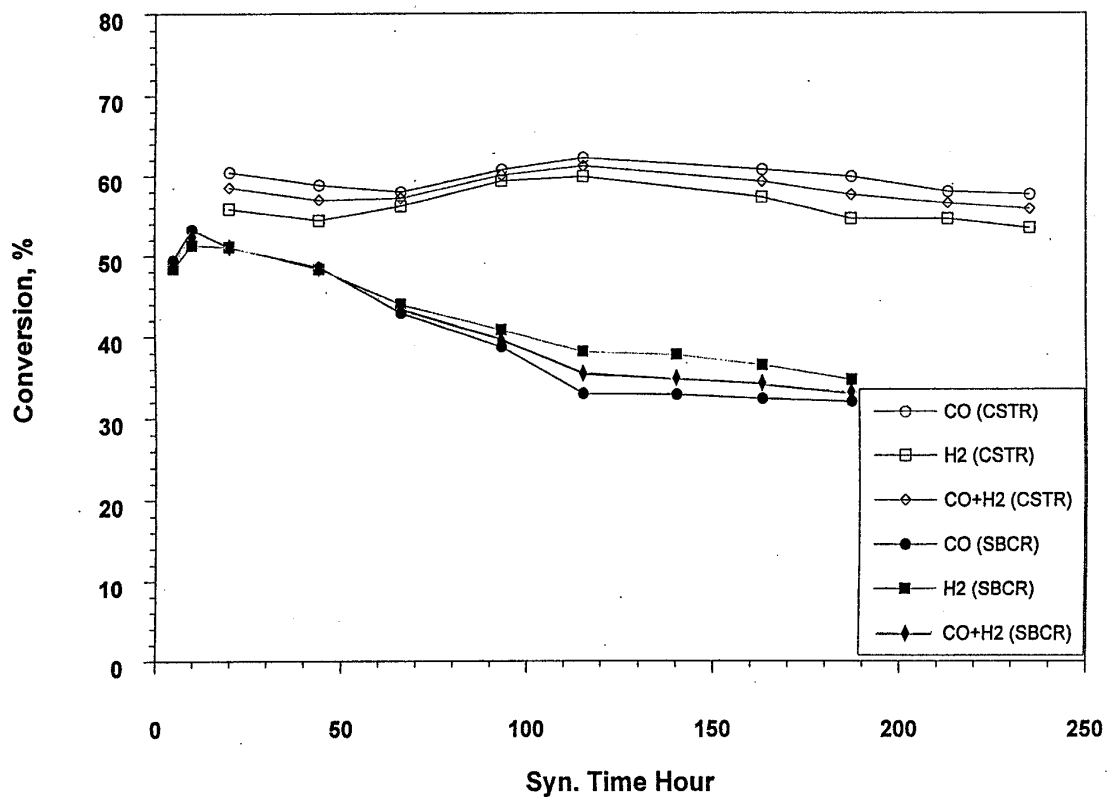


Figure 4. Conversion comparisons for the CSTR and SBCR systems.

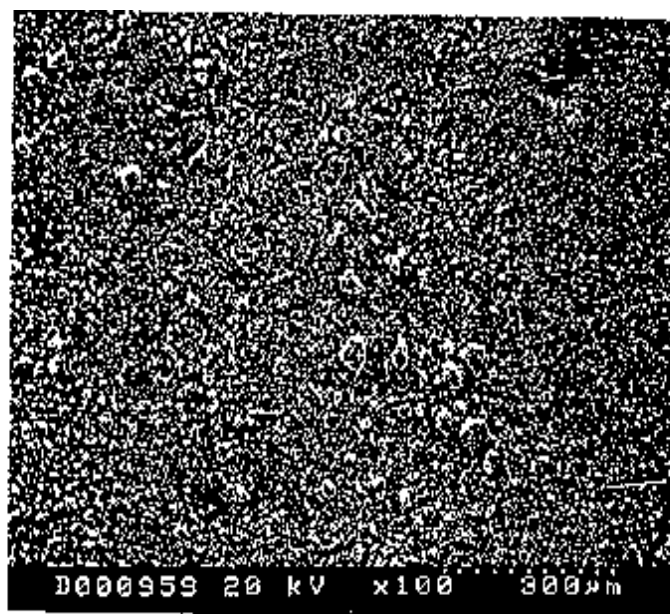


Fig. 5. SEM Scanning, the sample from the SBCR after synthesis 309 hrs.

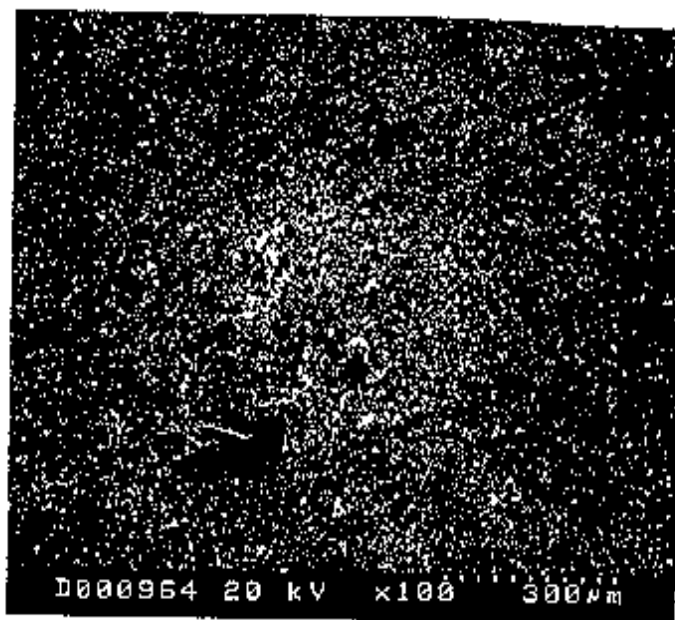


Fig. 6. SEM Scanning, the sample from the CSTR after synthesis 253 hrs.

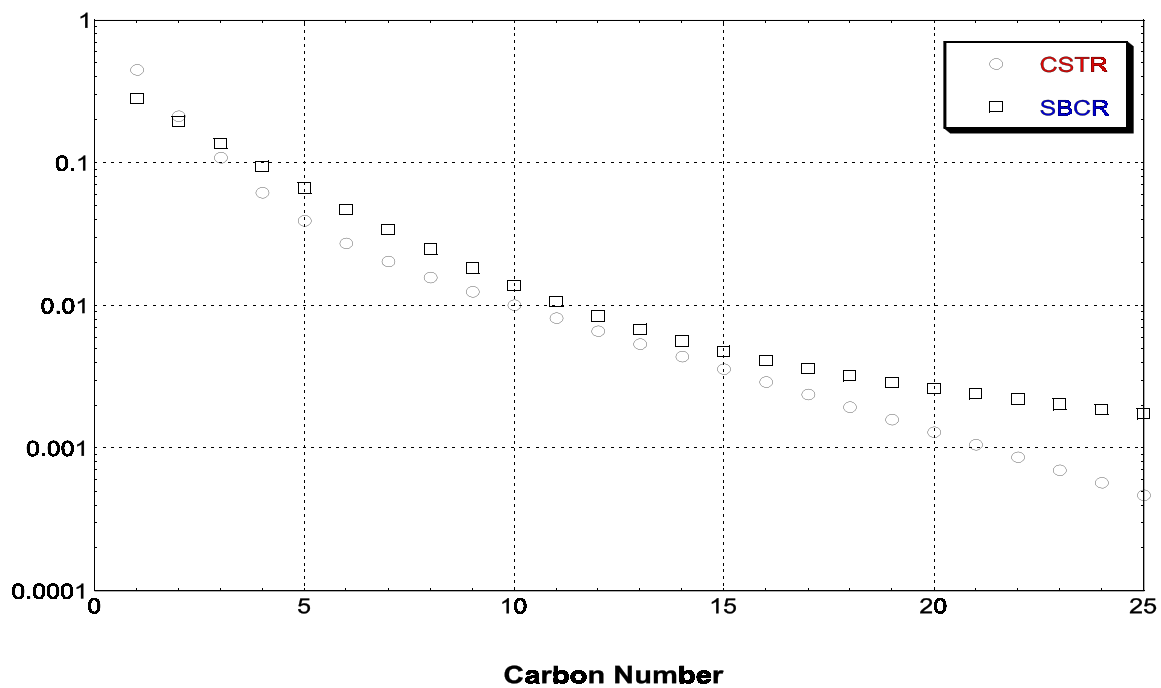


Figure 7. Comparison of the product distributions obtained in the CSTR and SBCR systems.

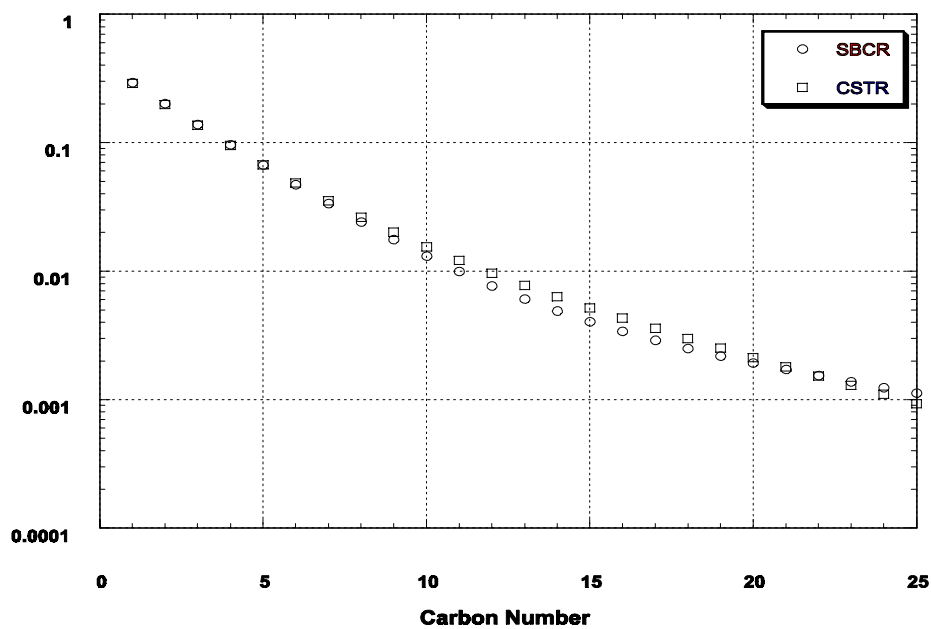


Figure 8. Comparison of the product distributions obtained in the CSTR and SBCR systems.

### **3.3.4 Additional Research**

#### **3.3.4.1. Verify the Quality of Data Obtained from the CSTRs.**

The previously unexplained loss and re-establishment of activity has been found to be due to the lowering of the liquid level in the reactor. The conversion data shown in Figure 1 clearly show the loss of activity when re wax (wax from the reactor) was collected on a daily basis in the first 500 hours of the run. When the sampling of the re wax was stopped the activity recovered to approximately the initial level. Repeating this cycle produced a loss and gain of activity again. From these data, it was suggested that removing the reactor wax lowered the liquid level by physically removing the wax material and thus allowed more of the lighter material including the start-up oil to be removed from the reactor. After most of the start-up oil was removed and the reactor contained a sufficient amount of FTS wax, the reactor liquid level became stabilized and sampling of the reactor wax could be done without affecting the activity.

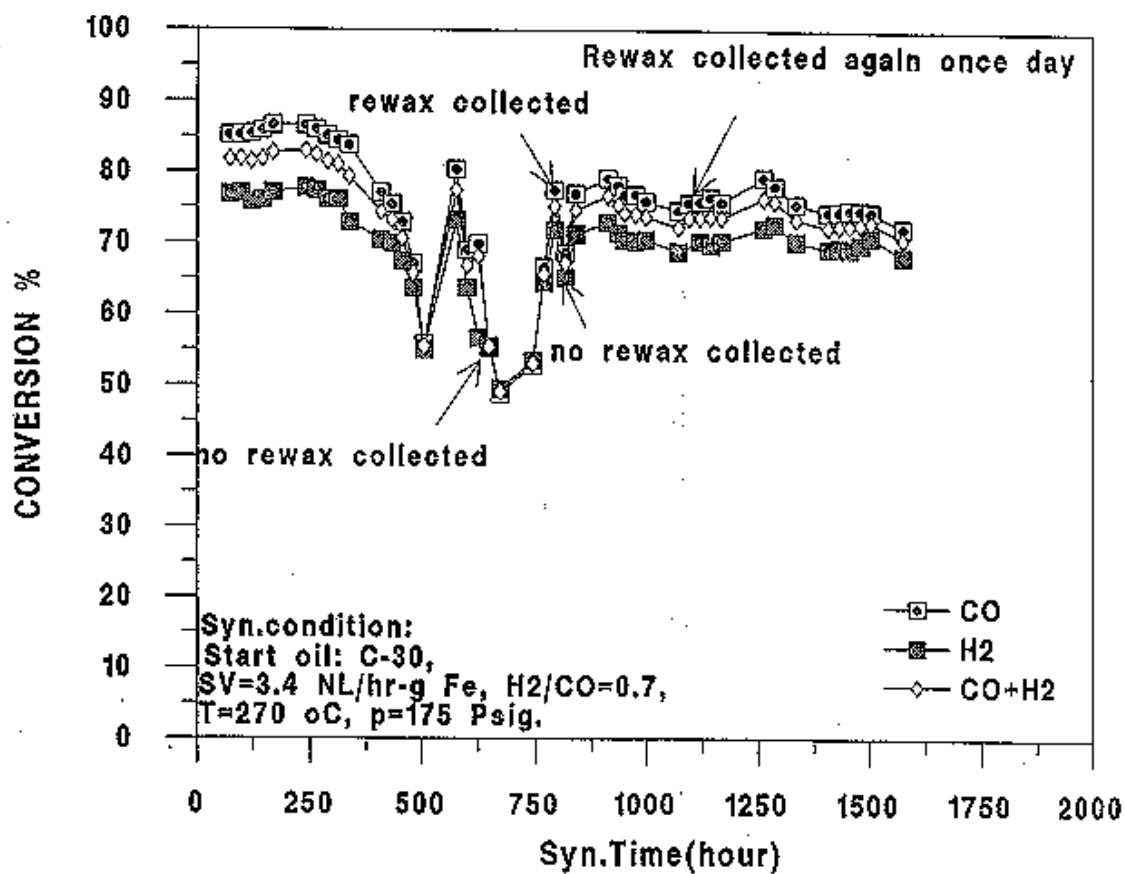


Figure 1. %CO conversion vs. Time on stream for runs LGX276-279 and LGX283 (4.4at%Al/3.0wt.%Cu/2.5-10.0wt.%K with  $T_{syn} = 230^{\circ}\text{C}$ ).

### **3.3.4.2 Comparison of Silica Based Hi-Alpha Catalyst at 230°C and 250°C**

#### **With C-30 oil at a 5.0wt% Catalyst Loading**

Two series of runs using five catalysts at synthesis temperatures of 250°C and 230°C were performed in the one liter continuously stirred tank reactors (CSTR). When Ethylflo C30 decene trimer was used as the start-up oil, a 5 wt.% catalyst slurry containing 15.3 g and 290 g of oil was used. When PW3000 wax was used, the initial slurry was 3 wt.% catalyst and contained 9.6 g of catalyst and 310 g of wax. For all the runs, the reactor solvent was C-30 oil with a catalyst loading of 5.0wt%. The iron-based catalysts used in these tests had been co-precipitated so that the atomic ratio of silicon to silicon + iron, i.e., [Si] / [Si+Fe], was at 0.044, or 4.4atomic(or mole)%. All the catalyst had been impregnated with copper such that the weight percentage of copper (relative to Fe) was at 3.0wt%Cu. Each of the five catalysts had a different amount of potassium present, specifically, 0.0wt%K, 2.5wt%K, 5.0wt%K, 7.5wt%K, and 10.0wt%K. As was the case for the copper, the potassium wt%'s are also relative to Fe. The list below shows the five catalysts tested and designates the atomic(mole) ratios of Si, Cu, and K, based on 100 atoms(moles) of Fe.

RJO228 (0.0wt%K) 100Fe:4.60Si/2.72Cu/0.00K

RJO229 (2.5wt%K) 100Fe:4.60Si/2.72Cu/3.66K

RJO230 (5.0wt%K) 100Fe:4.60Si/2.72Cu/7.52K

RJO231 (7.5wt%K) 100Fe:4.60Si/2.72Cu/11.58K

RJO232 (10.0wt%K) 100Fe:4.60Si/2.72Cu/15.87K

The first five runs performed were at 250°C and designated LGX236(0.0wt%K), LGX239(2.5wt%K), LGX240(5.0wt%K), LGX241(7.5wt%K), and LGX242(10.0wt%K). A comparison of the %CO conversion versus days on stream is shown in Figure 1. The



second series of runs, specifically LGX235(0.0wt%K), LGX244(2.5wt%K), LGX245(5.0wt%K), LGX246(7.5wt%K), and LGX247(10.0wt%K), was performed at the synthesis temperature of 230°C and the %CO conversion versus days on stream is given in Figure 2.

In general, the catalysts performed better in regards to CO conversion at the synthesis temperature of 250°C. At both temperatures, the catalyst run with the 5.0wt%K loading (RJO230) had the best CO conversion, while also for both temperatures, the 0.0wt%K loaded catalyst (RJO228) runs produced the poorest CO conversions. Again, for both temperatures, the catalysts at 2.5wt%K and 7.5wt%K (RJO229 and RJO231, respectively) produced comparable CO conversions, slightly lower than the CO conversion exhibited by the 5.0wt%K (RJO230) loaded catalyst runs, and the catalyst runs with the 10.0wt%K loadings were the fourth best with respect to the CO conversions, these also at both synthesis temperatures.

Note that for the 230°C synthesis conditions (Figure 2), the CO conversions for the 2.5, 5.0, 7.5, and 10.0wt%K loaded catalysts all fell within a 20% band at the start of the run and improved to a band of 10% or less by the end of the run. This band of CO conversions was also observed for the runs performed at 250°C, but only for the 2.5, 5.0, and 7.5wt%K loaded catalysts. The CO conversions were at ~80% for the 2.5, 5.0, and 7.5wt%K catalysts, while the CO conversion for the 10.0wt%K catalyst had a starting value of only ~50%. This justified another run using the 10.0wt%K catalyst, RJO232, at the synthesis temperature of 250°C. Run LGX250 was performed and the results of the CO conversion are given in Figure 3 and it can be seen that the %CO conversion did improve to values greater than 70%, with the exception in the drop of conversion starting at run hour 168 and reaching a minimum at ~run hour 264, which

was found to be due to a faulty inert gas valve. After corrective action was taken in regards to the valve, it can be seen the CO conversion did rebound and if these results were plotted with the 2.5, 5.0, and 7.5wt%K data, they would all fall into a band even tighter than that found with the 230°C CO conversions (i.e., bandwidth of ~10% CO conversion for the 250°C synthesis conditions).

Thus, in general, based on %CO conversions for these catalysts,

$$T_{\text{syn}} = 250^{\circ}\text{C} > T_{\text{syn}} = 230^{\circ}\text{C}$$

$$5.0\text{wt}\%K > 2.5\text{wt}\%K \cong 7.5\text{wt}\%K > 10.0\text{wt}\%K > 0.0\text{wt}\%K.$$

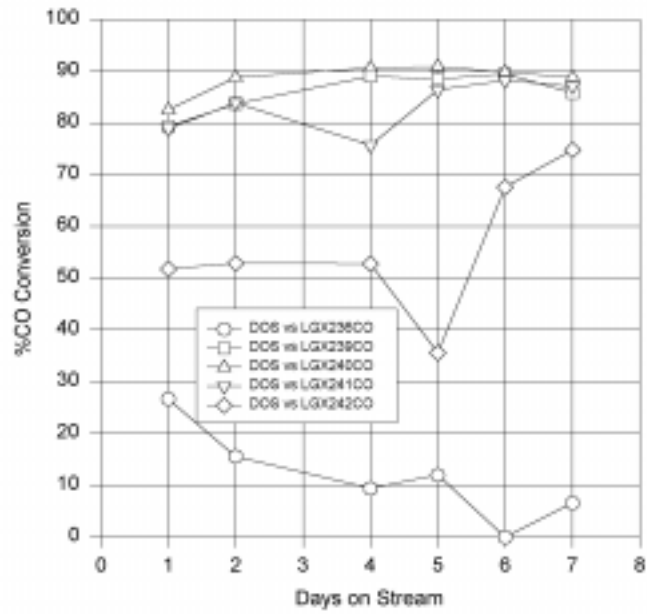


Figure 1. %CO Conversion vs Days on Stream for Runs LGX239-242 @ 250°C.

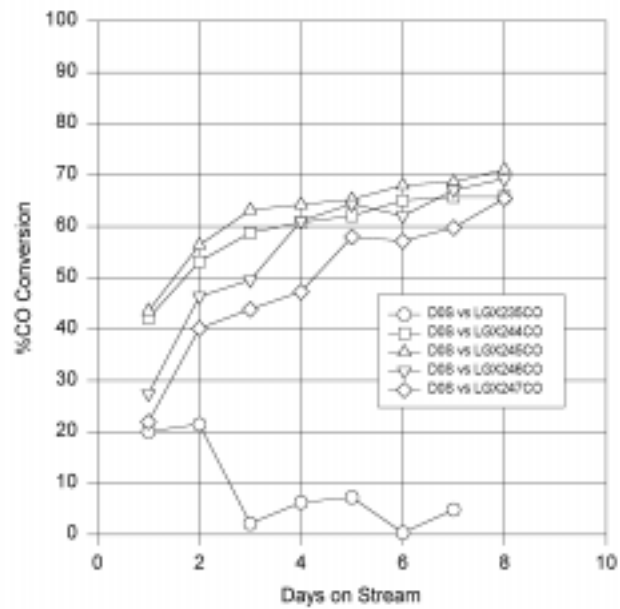


Figure 2. %CO Conversion vs Days on Stream for Runs LGX244-247 @ 230°C.

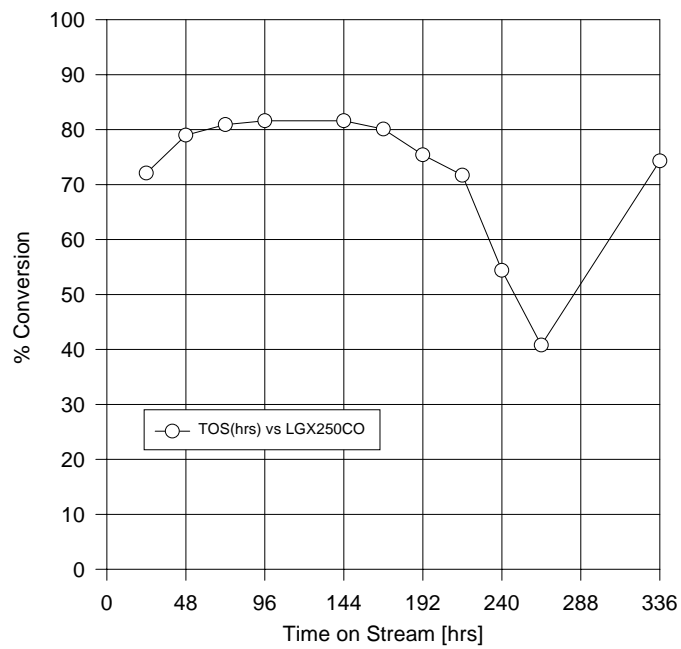


Figure 3. %CO Conversion vs Time on Stream for Run LGX250<sub>R7</sub> with  $T_{syn}$  @ 250°C.